Theoretical enhancement of the Gaussian filtering of engineering surfaces

David J Whitehouse

School of Engineering,
University of Warwick, Coventry CV4 7AL, UK

Taylor Hobson (Ametek) Ltd, Leicester, LE4 9JQ, UK.

Abstract

The present work is an extension of the current use of Gaussian filters to smooth surface texture waveforms. It suggests an extension using Hermite polynomials to improve the definition of boundary lines, and edges in the geometry of structured surfaces and to enhanced scratch and flaw detection.

Also, a new filtering concept is introduced to enhance the detection of boundary lines and edges and to improve the understanding of their local geometry thereby minimizing the uncertainties in structured surface filtering and characterization. How this approach can incorporate the measurement of free form surfaces as well as helping to improve the fidelity in scratch and crack detection, positioning and characterization is also discussed.

Key words.

Weierstrass transform, Hermite polynomials, Phase corrected filtering, surface metrology.

Structured surfaces, Free form surfaces, Scratch,crack and edge detection.

Nomenclature

D	Differential operator d/dx
f(x)	Profile signal from surface
F(ω)	Fourier transform of profile signal
g(x)	Gaussian statistical function $\exp(-x^2/2)$
G(ω)	Fourier transform of Gaussian statistical function
H_{enG}	Statistical Hermite polynomial applied to Gaussian function g(x)
H_{en}	Statistical Hermite polynomial
H_{nG}	Physical Hermite polynomial applied to Gaussian function g(x)
H_n	Physical Hermite polynomial

H_{DNG}	Output of profile convoluted with 'n'th differential
n	Polynomial degree, order of differential
t	Time
W[f](x)	Weierstrass transform involving function f(x) with Gaussian g(x)
W(x)	Weierstrass transform
x	distance along axis of profile
y	dummy height variable
ω	Spatial angular frequency
*	Convolution operation

1 General

1.1 Background

Earlier work, given in References [1,2], show the development of surface metrology filters from analogue filters through to digital phase-corrected filters having linear phase and amplitude transmission characteristics. These were deemed to be too difficult to implement at the time: wrongly as it happens, and a simpler method adopted. This was the proposition of the German members of ISO (International Standards Organization) who suggested that the transmission characteristic should be Gaussian in form.

A reason was that the Gaussian form can easily be generated in a computer by multiple convolutions of a 'box' moving average filter: three convolutions in fact being good enough to generate an impulse response which was within 1% of the true Gaussian form. One advantage of this shape being that this is also the form of its frequency response Fig 1. Unfortunately this nice relationship only holds for spatial-frequency relationships and not for spatial wavelength-frequency relationships.

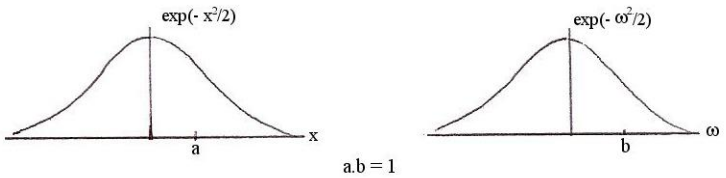

Fig 1 shows the Gaussian response and its Fourier transform. 'a' and 'b' correspond to the standard deviation positions of the two domains which are inextricably connected together by the relationship a.b=1.

Equation (1) relates the Gaussian signal and its transform (Figure 1), which are the same except for a factor of $\sqrt{2\pi}$.

$$\exp\left(\frac{-x^2}{2}\right) \Rightarrow \exp\left(\frac{-\omega^2}{2}\right) \quad (1)$$

A number of extra arguments could be put forward to support the Gaussian case. One was that the term was already very familiar in quality control circles and so would be readily accepted by the engineering community, Neither of these reasons was and is totally convincing enough to outweigh the linear version mentioned earlier. There was, however, a feature which did favour its use, which was that the amplitude probability function for abrasive processes such as grinding often had a Gaussian form, which introduced a level of symmetry between the amplitude and wavelength/frequency characteristics of the surface. Also, the Gaussian form is the basis of the Weibull distribution often used in fatigue, wear and product life, and so functionally it featured widely in engineering. The resulting weighting function for surface roughness emerged, therefore, as Equation 2, [4]

$$h(\alpha) = \frac{1}{\alpha_1 \lambda_c} \exp\left(-\pi\left(\frac{\alpha}{\alpha_1}\right)^2\right) \quad (2)$$

Where, $\alpha_1 = \sqrt{\frac{\ln 2}{\pi}} = 0.469$ and $\alpha = \frac{x}{\lambda_c}$,

x is spatial distance and λ_c is the cut off wavelength x. The cut-off value is at the 50% transmission point. This is the current situation regarding conventional filtering.

1.2 Recent changes in the filtering scene.

Recently, the filtering concept has changed by dropping the process control terminology e g waviness and incorporating a more general scale limited approach covering different scales of size introduced by a 'nesting' index. For this and other features of this approach see Ref [4].

The surface characterization situation has also changed dramatically because the geometric nature of surfaces is changing: free form surfaces with undefined geometry are being introduced to optimize functional performance and to reduce size, amount of material and hopefully cost and there is an explosion in the use of specific deterministic patterns and structures making up the surfaces. These include dimples, bosses, ridges etc in arrays or at random put on the surface to do a specific job. See Fig 2 for example. Even more disconcerting for characterization and filtering is the growing incidence of surfaces in which both types of new surface are present on one workpiece for different functional reasons. To tackle the problem of filtering these complex surfaces it seemed plausible to use the Gaussian filter as a starting point even if the only reason is because it is the basis of existing filters.

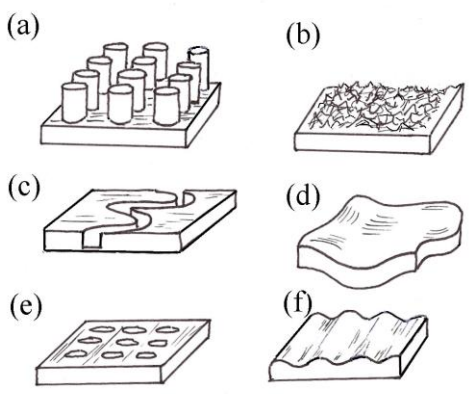

Figure 2 shows some typical types of surface to be measured: a, c ,and e are types of structured surface, b is a traditional machined surface, d is a free formed surface and f is a surface with waviness.

2 Enhancement of Gaussian filters

Note. In what follows the surface signal will be taken to be a profile obtained by a scan across an engineering surface using either a stylus instrument or an optical profilometer. The operator involving Gaussian derivatives developed below could, however, be applied in principle to any signal.

2.1 Weierstrass transforms

What is not known generally is that the smoothing of a function by means of Gaussian weighting function is in fact a special case of a Weierstrass transform given in Equation (3). This transform is already in the form of a convolution which makes it immediately applicable to such operations as smoothing and general filtering.

The transform is written in the form given below, where y is a dummy variable.

$$W[f](x) = \frac{1}{\sqrt{2\pi}} \int_{-\infty}^{\infty} f(x-y) \exp\left(-\frac{y^2}{2}\right) dy \qquad (3)$$

If the Weierstrass exponential has a standard deviation of σ then $\lambda_c/\sigma = 5.34$ and this gives the 50% transmission at the cut off λ_c of the Gaussian kernel used for surface texture filtering.

Equation 3 can be put in the more general form Equation (4), which corresponds to the convolution of the solution of Poisson's differential equation i.e., Green's function, with the surface profile, which corresponds with the filtering of the profile by means of the diffusion equation for free form surfaces [7].

$$W[f](x) = \frac{1}{\sqrt{4\pi t}} \int_{-\infty}^{\infty} f(x-y) \exp\left(-\frac{y^2}{4\pi t}\right) dy \qquad (4)$$

In this form the geometry smoothes as a function of time t in much the same way as heat diffuses throughout a body with time.

Under certain realistic conditions [5] the Weierstrass transform can be written in terms of a differential operator on the function *f(x)*, taken here as a surface profile.

$$W[f](x) = \exp\left(\frac{D^2}{2}\right) f(x), \text{ where } D = \frac{d}{dx} \text{ is the differential operator.} \quad (5)$$

W can in effect be expanded in terms of differentials [5]. It can also be inverted, again under certain conditions by the symmetrical expression (5).

$$f(x) = \exp\left(-\frac{D^2}{2}\right) \cdot W(x) \quad (6)$$

These formulae are very interesting because their relationships point to the use of a family of Gaussian differentials in the field of surface filtering; adding, in effect, a new dimension to characterization which is badly needed for the types of surface now being generated. These include structured and free form surfaces mentioned above which are being introduced to get optimum performance from parts and to control new manufacturing methods. New measurement technique and characterization are also needed in boundary and defect detection in particular on small and very smooth parts.

The problem set here is more difficult than when considering the requirements of earlier filters, which were designed almost exclusively to control manufacture. For the new types of surface the characterization does not necessarily follow conventional practice. New methods have to be explored for example using characterization which incorporates the spatial and the frequency domains together, such as in the Wigner distribution, rather than using either one domain or the other. This is because different features on one surface may need characterization for different functional reasons and consequently are best approached from different domains. For example the detection of the position of edges, shape of boundaries and their local geometry is likely to be important in the characterization of structured surfaces, whereas in free form surfaces a more general approach is necessary using for instance the diffusion equation which also points to Gaussian filtering [7]. This note explores the use of differential Gaussian filters, in particular to identify the boundaries of structured surfaces. As it is now becoming apparent that as more free form surfaces are incorporating structured surfaces on them, such as is shown in Figure 3 of a helicopter blade designed to prevent icing up, a joint approach capable of dealing with both types of new surface [8] is a real requirement for the future. The need extends also to the detection of various steps, lines, defects and flaws.

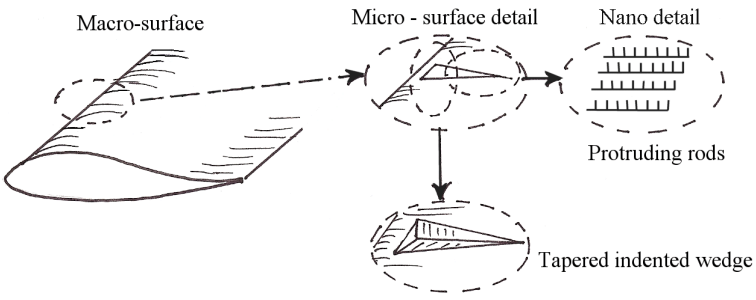

Figure 3 is an example of a blade where there is a macro form, which gets lift off, the micro wedges which channel the water back and up and over the foil and the bosses which form spherical droplets which then tend to fly off thus preventing icing up.

2.2 Measurement of basic features of structured surfaces and defects

There has been progress in the characterization of free form surfaces using the Gaussian filter in discrete form using the Laplace- Beltrami method applied by Jiang [7] in which the value of the curvature at a point on a free form surface evolves in a direction normal to the surface at that point i.e. it can possibly relate to those key parameters which determine much of the functionality of the surface. In the time version corresponding to Green's function in Equation 4 the geometry effectively diffuses in time analogously to the temperature field in heat conduction [8].

Nothing in this treatment helps in the measurement of structured surfaces. By their very nature they imply boundaries, which in surface terms implies steps edges ridges etc. Measurement is required to establish the precise nature, position and the extent of such boundaries. The basis of a system to detect geometric characteristics could in the first instance comprise simply of the differentials of Gaussian operators but the question arises as to whether this is adequate. Patterns and relationships between various parts of the structure on a surface cannot be built up without accurate boundary detection and a knowledge of line and edge geometry: they are the very foundation of structured surface characterization.

The other important area in which the filters need to be enhanced is in flaw and defect detection and characterization. The reason for such a need is that in the semiconductor industry and increasingly in thin films for optics and coatings in manufacture surface defects can be catastrophic. Any way in which scratches, cracks and pits can be detected, measured and their position correctly registered has to be beneficial to functionality. Current filters do not meet this need. In what follows some new ways of developing filters will be discussed in which the uncertainty of measuring and estimating these difficult features will be introduced.

3 Gaussian differentials for boundary assessment using statistical Hermite polynomials

First and second differentials have been used to detect changes in intensity of parts of pictorial images [9] . The first differential of the received light shows a change in intensity as a peak whereas the second differential shows it as a zero crossing. Investigating boundaries on structured surfaces in this way is different because it is real geometry which

has to be measured, which brings in extra variables associated with their curvature and form and the interaction of the instrument with the surface.

In terms of surface geometry the options for differentials, using the usual form for differentiating convolutions, are

$$\frac{d^n}{dx^n}\left(f(x)*g(x)\right)=g(x)*\frac{d^n}{dx^n}f(x) \quad \text{or} \quad f(x)*\frac{d^n}{dx^n}g(x) \tag{7}$$

Of the two the last is to be preferred because the differential form is known in advance.

In terms of the Hermite polynomials Equation 7 becomes

$$\frac{d^n}{dx^n}f(x)*g(x)=(-1)^n f(x)*H_{en}(x)g(x) \tag{8}$$

In Equation 8 the n=0 case corresponds to the Weierstrass n=0 case and the n=1 and 2 correspond to the Gaussian differentials for the structured surface case where $H_{en}(x)$ are the statistical Hermite polynomials, giving the set as

$$\begin{array}{ll} f(x)*g(x) & \text{for n = 0} \\ f(x)*x\cdot g(x) & \text{n = 1} \\ f(x)*\left(x^2-1\right)\cdot g(x) & \text{n = 2} \end{array} \tag{9}$$

These correspond to the moments of the Gaussian kernel and form an orthogonal set which is useful in analysis

For areal rather than profile data the n=2 case is Equation (10).

$$f(x,y)*\left(x^2-1\right)\cdot\left(y^2-1\right)\cdot g(x,y) \tag{10}$$

4. Joint characterization of profile and transform using Alternative Hermite Differential Equation and application to boundary assessment

Equation 1 shows an example of when the form of the filter weighting function and its Fourier Transform are the same, in this case Gaussian. It can be shown that this form is an optimum for specifying joint characteristics with a minimum of uncertainty. This conclusion is reached using entropy considerations and Heisenberg's Uncertainty Principle [10]

The general relationship between the spatial and frequency signals usable for surface characterization is given by transforming Equation 7. Thus

$$\frac{d^n}{dx^n}\left(f(x)*g(x)\right)=f(x)*\frac{d^n}{dx^n}g(x) \quad \Rightarrow \quad F(\omega)\cdot\frac{d^n}{dx^n}G(\omega) \tag{11}$$

The spatial and frequency equations can only have the same form when $H_{DGN}(x) = f(x) * \frac{d^n}{dx^n} g(x)$, is the output of the profile convoluted with the 'n'th differential of the Gaussian function, and the differential equation (12) (called here the Alternative Hermite Differential Equation) is obeyed.

Then,

$$\frac{d^2 H_{DNG}}{dx^2} - \left(x^2 - (2n+1)\right) H_{DNG} = 0 \qquad (12)$$

i.e. $f(x) * \left(\frac{d^2 g(x)}{dx^2} - \left(x^2 - (2n+1) g(x)\right) \right) = 0$

Hence, $\frac{d^2 g(x)}{dx^2} - (2n+1) g(x) = 0$, which has the solution $g(x) = H_n(x) \cdot \exp\left(-\frac{x^2}{2}\right)$

where $H_n(x)$ is the 'physical' Hermite polynomial, not $H_{en}(x)$ the 'statistical' version of the Hermite polynomial, which means that the solution to equation 12 does not involve the differentials of the Gaussian function directly and the $H_n(x)$ polynomials are not the moments, as are the statistical Hermite polynomials, but the polynomials are the same for frequency as they are for space, so there is an exchange of benefits.

However, the direct differentials and H_n are related by Equation 13.

$$\left[x - \frac{d}{dx} \right]^n \exp\left(-\frac{x^2}{2}\right) = H_n(x) \exp\left(-\frac{x^2}{2}\right) \qquad (13)$$

From which it emerges for the case of n=2 that

$$H_{2G}(x) = 4H_{e2G}(x) + 2 \qquad (14)$$

This gives the relationship between the two forms of second differentials; the conventional one H_{e2G} and the one H_{2G} obeying the Alternative Hermite Differential Equation 12, which preserves the same form as its Fourier transform. (The G is included in the suffix to indicate that it will be operating with the Gaussian function). If H_{D2G} is the result of a convolution with the function *f(x)* then

$$H_{D2G}(x) = f(x) * [4H_{e2G}(x) + 2] g(x) \quad \Rightarrow F(\omega) \cdot [4H_{e2G}(\omega) + 2] G(\omega) \qquad (15)$$

i.e. $H_{D2G}(x) = f(x) * H_{2G}(x) \cdot g(x)$,

where the right hand side of Equation 15 is the Fourier transform of the left hand side. Obviously the square bracket in equation 15 has been normalized by a factor two to make the value of the weighting function at the origin equal to unity to give the impulse unit strength

in both cases. This normalization can be achieved without any loss of obedience to the Alternative Hermite Differential Equation 12, making Equation 15 now

$$H_{D2G}(x) = f(x) * [2H_{e2}(x) + 1]g(x) \quad \Rightarrow \quad F(\omega) \cdot [2H_{e2}(\omega) + 1]G(\omega) \tag{16}$$

Figure 4(a) illustrates the difference between the two Hermite Gaussian differentials of Equation 15. The forms are shown inverted for clarity. Both clearly have the second differential form: the $H_{e2\ G}$ central lobe has an area equal to the sum of the areas of the differential lobes whereas in the case of H_{2G} the differential lobes each have twice the area of the central lobe! In effect the smoothing has been degraded and the differential enhanced near to the origin. The H_{e2G} is a straightforward second differential whereas H_{2G} is not. In fact when operating on a Gaussian function it becomes it is a combination of a differentiator, a filter and an amplifier! This is what makes it potentially more useful.

Figure 4 not only shows the difference in shape, it also compares the spatial and frequency characteristics. Notice that the frequency form for the H_{e2G} is not the same as that its spatial form, unlike H_{2G} which does have the same shape, because it obeys the Alternative Hermite Differential Equation and as a result has different frequency characteristics relative to the standard differentials!

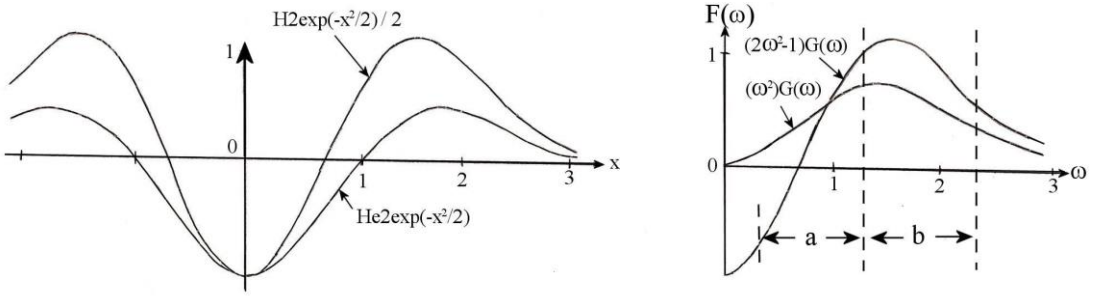

(a) Spatial comparison- impulse responses (b) Frequency comparison

Figure 4 Comparison of Gaussian Hermite differentials

5. Discussion

5.1 General

The fact that the operator $H_{2G}g(x)$ on the profile signal and its transform have the same form means that the same operator can be applied to both; one as a convolution and the other as a multiplier. The impulse response Figure 4(a) shows that the position of any boundary line or scratch will be better defined using the new method H_{2G} because the central pulse is sharper than that of the $H_{e2}g(x)$: it has over twice the curvature and in the frequency domain it is obvious in region 'a' that it is a far better differentiator than the second differential, and that the high frequencies in region 'b' will be revealed with higher fidelity as the transmission is close to unity in value, thereby giving a better idea of the crack or edge geometry e.g. possible changes in curvature. For higher frequencies there is a better smoothing of the,

usually noise, frequencies because of the bigger lobes near to the origin in Figure 4(a). So, for the impulsive nature of any signal this new method is superior. On the other hand by using this strategy to enhance the differential operator negative frequency content has been introduced near to the origin, which will distort the low frequencies, as seen in Figure 4(b). This is acceptable because the low frequency content of structured surfaces is invariably small when compared with the magnitude of the structure. For scratches and cracks the sharper slope of the frequency curve, which is what is being sought by the method will reduce the uncertainty of the position and increase the ability to detect the crack, but will enhance pile-up shape, and care will have to be taken not to mistake this for real material. This effect will be present in any differentiator but it will be considerably magnified by using this method.

5.2 Step response

The situation is not quite as obvious for the step responses shown in Figure 5 because although the new system has a slightly sharper slope it does not have a zero crossing, but it has closer extrema surrounding the edge which gives less uncertainty of the possible edge position i.e. the uncertainty is reduced from u_2 to u_1 a factor of about 2:1. It could be that the H_{e2G} could be used to locate the edge by means of the zero crossing and the H_{2G} to establish the maximum uncertainty.

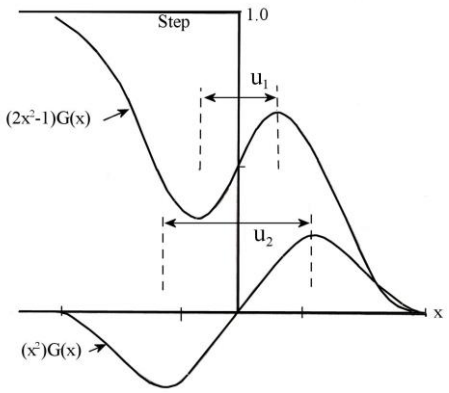

Figure 5 Comparison of step responses of $H_nG(x)$ and $H_{en}(x)G(x)$. (The height of the step has been normalized by $\sqrt{2\pi}$ in the figure).

The advantage of having symmetry between the spatial and frequency characteristics given by equation 15, over the simple Gaussian differentials, is that the higher frequencies of the scratch, crack or ridge edge are revealed with higher fidelity and have more discrimination of the boundary or line.

5.3 Defect detection

Defect detection is a vital engineering requirement in many areas such as on semiconductor wafers and in aerospace for example where scratches on engineering parts can be detrimental to performance especially in high stress situations such as near the root of a turbine blade.

The use of these filters to assess defects is best revealed using stylized profiles. Figure 6 shows how a wedge like profile, which corresponds to a scratch defect Fig 6(a) and a square trough in Figure 6(b), which corresponds to a boundary gap or a crack defect respond to the enhanced H_n and current H_{en} filters.

Some general comments.

In both cases (Fig. 6) it is clear that the frequency characteristics of the Hermite H_n function as (i), in the right hand figures have very much the same shape near to the origin as the frequency characteristics of the geometry being measured shown in (iii) on the right hand side. Notice also that the spatial response of the two filters to these standard benchmark profiles for defects are quite different: The conventional H_{en} filter responses to the scratch and gap geometries (ii) is quite muted when compared with the H_n filter responses (i) which highlights the features much more prominently in height and give them a sharper slope. In effect its side-lobes, in the spatial response, can 'flag up' the presence of the defect much more easily than the case of the $H_{e\ n}$ function. Also, as the correlation of the frequency characteristic curves (i) and (iii) near to the origin is high, any changes in form of the ridge geometry due to a flaw should be spotted. See Figure 8.

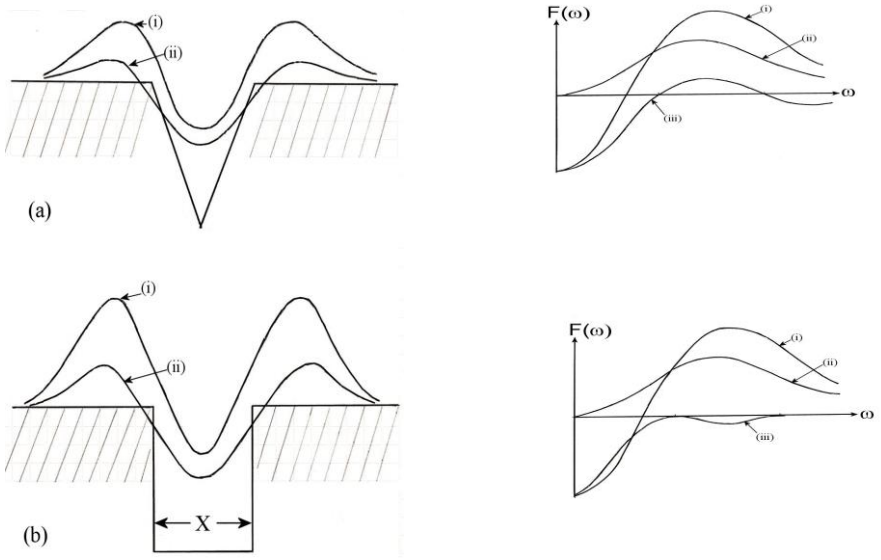

Figure 6 Responses of the two filters to a wedge like scratch (a) and to a trough depression representing a boundary gap or a crack (b). Left figures; (i) $H_n\ G(x)$ spatial response (ii) $H_{en}G(x)$ spatial response. Right figures; (i) $H_n\ G(x)$ frequency response, (ii) $H_{en}G(x)$ frequency response. (The frequency responses of the scratch and crack are shown as (iii)

(normalised) and their abscissa is normalised relative to $2\pi/X$ where X is the width of the scratch and crack features).

How the enhanced filter works could be used as a tool in quality control is demonstrated by means of the standard scratch profile on Figure 7. There are three things which need to be carried out in order to satisfy defect quality control. These are that the scratch or crack defect has to be detected, then its exact position on the surface has to be determined, which usually means that the deepest point has to be identified and finally the defect has to be characterized i.e. classified. As the scratch or crack is mainly in the subsurface its geometry has to be amplified by the detecting mechanism so that it is not swamped by extraneous noise. This is achieved by the filter responding vigorously, by producing large side-lobes, wherever there are scratch or crack edges in the profile as seen in Figure 7(a). The position of the defect has to be pinpointed accurately because this determines its hazard level: too close to the root on a turbine blade can cause a fatigue crack to form so it has to be located properly i.e. not just the crude position obtained from the scan. Fine position is obtained from the central lobe of the filter because the centre of curvature of the lobe points directly to the deepest point as seen in Figure 7(b). It can be seen from the figure that on both counts the enhanced filter is better than the currently used Hermite filters used for pattern recognition[11,12,13]which do not satisfy the differential equation proposed here.

The key point is that the two of the three factors needed for defect quality control namely detection of the defect and its position, can be satisfied using this filter because of its enhanced side lobe amplitude for the former and the sharper central lobe for the latter.

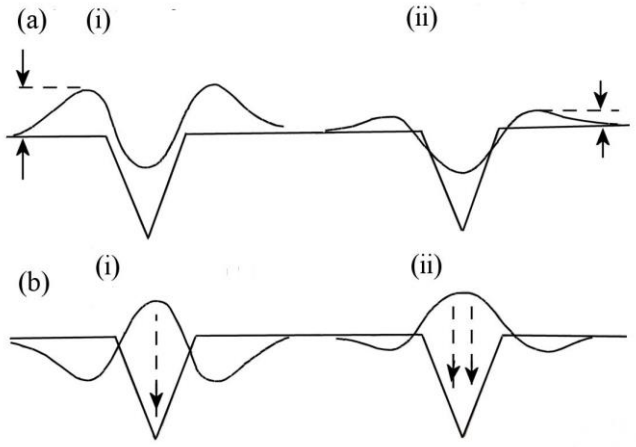

Figure 7 shows a comparison between the behaviour of the enhanced filter (i) and the current filter (ii) for (a) *detection*, shown with arrows indicating the prominence of the lobes and (b) *positioning*, showing dotted lines with arrows indicating uncertainty in the location of the critical part of the scratch or crack. On both critical criteria the enhanced filter is superior.

The third aspect of control i.e. characterization, requires the ability to see detail within the profile of the defect. Figure 8 shows how, to some extent, this is possible with this filter yet not with the current Hermite filter.

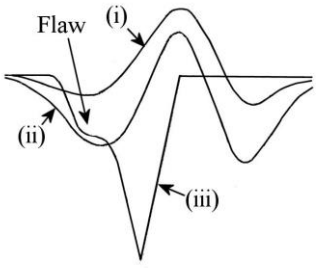

Figure 8 shows the response of the two filters to a flawed scratch. (i) current Hermite H_{en} ,(ii) enhanced Hermite H_n , (iii) flawed scratch profile.

Figure 8 shows a scratch with a flaw in the shoulder. The enhanced filter $H_n(x)G(x)$ shown as (ii) reveals the general flaw shape while maintaining the fidelity of the edge detection whereas the current Hermite filter $H_{en}(x)G(x)$ shown as 8(i) is quite impervious to the flaw in the scratch profile so any attempt to characterize the scratch using it would be impossible. Incidentally, the curvature of the peak of the central lobe, of the enhanced filter is more than twice that of the other filter and hence has better position discrimination.(See Figure7 (b)(i)). Also, the lobe structure of H_n is closer to those of a fourth differential than a second differential which makes it more capable of seeing local shape i.e. flaws (Figure 8). The fact that it has three lobes in this distinct configuration rather than the standard lobes of the other Hermite- like filters guarantees some advantage.

Obviously the effectiveness of this new method depends on the particular spatial bandwidth of the scratches and cracks present on the surface but this proviso applies to any type of filter. The fact that the detection lobes of the enhanced filter are of the same order of height as the defect itself means that peak to valley noise levels in the general signal of about six times the defect depth should not bury the defect. This should be about three times better than for the other filter which has much smaller side-lobes!

The unusual feature, which is made possible by the symmetry between space and frequency domains due to obeying the modified Hermite equation, is that the H_{2G} filter has a higher slope in both the frequency and the spatial domains which gives a better discrimination in both domains, which in turn means less uncertainty in two critical factors of the boundary; the geometry of the scratch or crack and its position.

Note that the responses shown in these figures are shown in two modes: one the vertical mirror image of the other as in Figure 7(a) and 7(b). The upper mode could be regarded as the detection mode and the lower the position mode of the response. They are exactly the same response in different guises.

Finally, both the frequency term and the spatial term in equation 15 are fundamental to structured surface characterization. However, there is another observation which is that the components in the square bracket term relate to both structured surfaces and free form surfaces. Thus, equation 15 in effect comprises of two components

$$2H_{e2}(x)\exp\left(-\frac{x^2}{2}\right) = 2\left(x^2-1\right)\exp\left(-\frac{x^2}{2}\right) \quad \text{to examine for boundaries, i.e. edges, lines etc}$$

$$\text{and } \exp\left(-\frac{x^2}{2}\right) \text{ to match up with any free form filtering via Laplace - Beltroni} \qquad (16)$$

This ties in with the Weierstrass transform comments made earlier (Equation 4).

Both can be utilized when the surface geometry contains both free form elements and structured surfaces as in the case of the helicopter blade shown in figure 3.

The first differential and other differentials can be treated in the same way.

For the first differential the equivalent relationship to equation 15 is given by

$$H_{D1G}(x) = f(x) * (-1)\cdot H_{1G}g(x) \quad = \quad f(x) * (-1)\cdot 2xg(x) \qquad \Rightarrow \quad F(\omega)\cdot 2\omega G(\omega)$$

However, there is no extra benefit in spatial or frequency aspects in going to the H_1 as just the factor 2 is involved.

5.4 Summary.

Differential Gaussian filters have been used for direction-following in pattern recognition [9], edge and line detection [11,12]. Filters involving first order differential Hermite polynomials have been used recently in optical image analysis such as in refs [13,14], but not the enhanced second order as in this report. Differential filters have been used in defect detection [15] but not with any Hermite aspects. The vast majority of advances in filtering has been in the implementation of digital algorithms associated with areal pattern recognition and not with the basic theory associated with the filters as is the case here. Problems associated with the detection and the classification of defects have been reported in [16].

This approach reveals that there are two aspects to this work involving Gaussian filtering. One is the realization that the use of the ISO Gaussian filter for engineering surface metrology [17] should be extended to include its differentials in the form of statistical Hermite polynomials in order to be able to characterize and measure structured surfaces and to detect and position defects. The other is that it is possible to use a mathematical stratagem, involving the physical Hermite polynomials, to enhance this capability by artificially distorting the space and frequency domain characteristics of the filter in order to magnify the basic structure features such as lines, ridges and edges from which the patterns of structured surfaces can be built up, and the ability to detect and position scratches and cracks improved.

There has been no previous use of the technique revealed here involving the use of the alternative Hermite differential equation 12 to develop a filter for signal analysis.

6. Conclusions

1. The International Standards Organization 4287 Gaussian filter specification should be expanded to make it more able to characterize surface defects and structured surfaces. The forms explored in this paper could be the foundation for the additions.

2. There have been great strides in scanning methods for areal measurement of surfaces and for pattern recognition but not so much for interrogating the instantaneous received signal. Simple differentiation for intensity changes have been the norm. The technique outlined above may be a step forward as it provides extra smoothing for the higher frequency noise at the same time as better resolution of line boundaries.

3. As this technique enhances scratch and crack detection, position and definition it could assist in defect control on critical engineering parts such as turbine blades.

4. Using the Alternative Hermite Differential Equation to develop a differential Gaussian operator may be a basis for a unique way of detecting and measuring surface boundaries and minimizing their uncertainties.

5. Future work will be to verify the practicality of the theory given above for structured surfaces and if possible defects. Also, work to extend the theory to measure and classify free form surfaces, possibly using derivatives of the Weierstrass transform, will be undertaken. This investigation could form a framework for measuring and characterizing both types of new surface in one package and having the extra capability of detecting defects.

References

[1] Whitehouse D.J. and Reason R.E. (1965) 'Equation of mean line of surface texture found by an electric wave-filter' (Rank Organization, London).

[2]Whitehouse D.J. (1967)'Improved type of wave-filter for use in surface – finish measurement' Proc. Inst. Mech. Eng. Vol. 182 Pt 3 K pp 306-319.

[3] BSI 1134, 1963, British Standards Institute London W4 4Al

[4] ISO/TS 16610-61, ISO 4287 1997. International Standards Organization P.O.box 56 CH-1211 Geneva 20.

[5] Bilodeau G.G.(1962) 'The Weierstrass Transform and Hermite Polynomials' Duke Mathematical Journal Vol. 29 pp 293-308.

[6] Jiang X. ,Cooper P., & Scott P.J. (2011) 'Free form surface filtering and the diffusion equation' Proc Roy Soc A 467 pp841-859

[7] Whitehouse D.J. (2012) 'Surface geometry, miniaturization and metrology' Phil. Trans. R. Soc. A, Vol. 370, 3829-3830.

[8] Carslaw H. S. and Jaeger J.C. (1959) 'The Conduction of Heat in Solids' Second Edition (Clarendon Press. Oxford)

[9] Marr D and Hildreth E (1980) 'Theory of Edge Detection' Proc. Roy. Soc. Lond. B vol 207 pp187-217

[10] Leipnik R. (1959) 'Entropy and the Uncertainty Principle', Information and Control Vol 2 pp 64-79

[11] Gerig G, (2010) 'Canny edge and line detection' CS/BIOEN 6640 www.sci.utah.edu.

[12] Gerig G, (2012) 'Edge detection' CS/BIOEN 4640 ibid.

[13] Estudillo-Romero A.and Escalante- Ramerez B. (2008). The Hermite transform; an alternative image representation model for Iris recognition' Progress in Pattern Recognition, Image Analysis and Applications Vol 4 Issue 1 pp 79-82.

[14] . Pavelyeva E.A., Krylov A. S. (2010) An adaptive Algorithm of Iris Image Key Points Detection www.graphicon.ru/html/proceedings/2010/conference/biometry/119.pdf

[15] Choi S.H. Yun J P , Seo B, Park YS and Kim S.U., (2007) 'Real time defects detection algorithm for high speed steel bars'. Proc World Ac.Sc.Eng Tech Vol 21 ISSN1307-6884

[16] Rahaman G M A and Hossain M M (2009) 'Automatic defect detection and classification technique from image' Int. Journal of Computer Science and Information Security' Vol 1 no 1pp 22-30

[17] ISO 25178-pt2 (2012) Surface texture: Areal - Part 2: Terms, definitions and surface texture parameters. International Standards Organization P.O.box 56 CH-1211 Geneva 20.